J Braz. Soc. Mech. Sci. Eng. (2015) 37:285–296
DOI 10.1007/s40430-014-0173-8

TECHNICAL PAPER

Hydrodynamic considerations on the performance of chilled water thermal storage tanks in the discharge cycle

M. M. Milaré · M. S. Rocha · J. R. Simões-Moreira

Received: 16 October 2013 / Accepted: 25 February 2014 / Published online: 13 April 2014

Abstract The paper analyzes the effect of hydrodynamic viscous boundary layer growth over the performance of a thermal storage tank during the discharge cycle. As well established in Fluid Mechanics textbooks, a viscous boundary layer modifies the velocity profile across the tank section. Consequently, in a discharge cycle the warm water flowing outside the boundary layer (i.e., in the core region) reaches the tank bottom exit faster than that if the down flow water were flowing at the mean velocity based on the discharge flow rate, which is the usual designing and tank selection assumption. Consequently, the storage tank height must be greater than that determined using the simple mean flow velocity. Two controlling parameters appear naturally in the analysis: the Reynolds number based on tank diameter, $Re_{Ø}$, which is also associated with the hydrodynamic entry length, and f, which defines the position of a given contact surface from the tank entrance to the hydrodynamic entry length. Results show that the tank loss of capacity due to viscous effects may not be negligible and the selection of a height-to-diameter tank ratio is essential for minimizing those effects.

Technical Editor: Jose A. dos Reis Parise.

M. M. Milaré
Masterplan Engenheiros Associados Ltda, São Paulo, Brazil

M. S. Rocha
IPEN-CNEN/SP, Nuclear and Energy Research Institute, São Paulo, Brazil

J. R. Simões-Moreira (✉)
SISEA - Alternative Energy Systems Laboratory, Mechanical Engineering Department, Escola Politécnica at University of São Paulo, Av. Prof. Mello Moraes, 2231, São Paulo, SP 05508-900, Brazil
e-mail: jrsimoes@usp.br

Keywords Thermal storage · Chilled water · Tank storage, loss of capacity

List of Symbols

c	Specific heat (J kg^{-1} K^{-1})
E_i	Internal energy due to the difference between the thermal load and chiller capacity (J)
f	Dimensionless position computed from the boundary layer starting region
g	Gravitational acceleration (m s^{-2})
H_{lb}	Loss of capacity (m)
H_{lm}	Equivalent height loss due to water masses mixing (m)
H_u	Useful height (m)
r_0	Tank internal radius (m)
Re	Reynolds number
Ri	Richardson number
t	Time interval (s)
T_c	Chilled water temperature (K)
T_h	Hot water temperature (K)
U	Axial velocity (m s^{-1})
V_u	Useful tank volume (m^3)
x	Contact surface distance from boundary layer beginning hydrodynamic entry length (m)

Greek symbol

β	Thermal expansion coefficient
δ	Boundary layer thickness (m)
δ^*	Relative thickness
Δ	Displacement of viscous contact surface (m)
ϕ	Tube diameter tank diameter (m)
ρ	Density (kg m^{-3})

Subscripts

0	*Mean*
1	Initial time

2 Final time
c Chill
el Entry length
h Hot
i Time interval
l Laminar flow
lb Additional loss
lm Equivalent loss
lo Actual displacement
n Total number of time interval
ol Overall displacement
t turbulent flow
u Useful

1 Introduction

Thermal storage technology is generally used in air-conditioning systems for supplying chilled water to meet a building cooling load during daytime (peak period) when electricity cost is high. In other configurations, thermal storage systems are also used in combination with electrical chillers of lower capacity to supply the overall cooling load. As a general rule, in any situation, chilled water is usually produced overnight when electricity price is lower. Thermal energy storage technology based on chilled or warm water, and ice bank, provides operational cost savings along with operating system flexibility enhancement [1, 2].

Sensible heat thermal storage systems are primarily a considerable volume of low temperature water usually stored in cylindrical tanks of vertical configuration. According to the ASHRAE [3, 4], vertical tanks are widely used in thermal storage installations because of their simplicity of operation, low capital costs, and high working efficiency. The fundamental working principle relies on the hot and cold water density difference, which enables a region of separation between warm water (top) from the chilled water (bottom) within the tank, a phenomenon known as thermocline. To avoid disturbances and undesired chilled and warm water mixing, water inflow and outflow run smoothly through diffusers installed at the bottom and at the tank top. Diffuser types frequently used are the radial and the octagonal ones. A radial diffuser is made of a parallel disk mounted next to the surface from which water is to be distributed; octagonal ones are made of one or two sets of rings built from tubes on which there are equally spaced slots composing the water distribution system.

Tank storing loss of capacity, despite occurring in the charging and discharging cycles which induces the formation of a thick layer between chilled water and returning (warm) water, is called thermocline. Many important studies have been carried out to verify the main mechanisms that contribute to thermocline formation at the field operational conditions. Parametric analyses were performed by theoretical and experimental studies to understand all the physical variables that are involved in the problem.

A numerical analysis of storage tanks has been reported in the specialized literature, mainly for transient behavior of thermocline formation and tank storing efficiency, as mentioned by Li et al. [5].

Dimensional analysis is a valid tool to understand the thermal and hydrodynamic mechanisms involved in such a problem, and it has been used to correlate the several parameters that control the tank loss of capacity, and the main causes are extensively discussed in the technical literature. It is a consensus that the inlet diffuser operation is very important to tank loss of capacity and, therefore, most previous studies have been concentrated on analyzing that device influence during charging and discharging cycles.

According to Wildin and Sohn [6], the tank loss of storing capacity is intrinsically related to the thermocline instability, and a further mechanism can be explained by two dimensionless parameters considered during the charging phase: the initial densimetric Froude number and the inlet Reynolds number. The densimetric Froude number can explain the ratio of inertia and buoyance forces to produce the gravity-driven motion, which is preferable in the tank charging phase, preventing vertical motion from causing instabilities in the thermocline formation. The inlet Reynolds number associated with the inlet fluid inertia also contributes to the instability formation in the region below the thermocline. Those authors conducted experimental tests to verify the gravity current and inlet fluid effects over the thermocline formation.

Also, as discussed in ASHRAE [3], experimental work suggests that the diffuser influence over water mixing occurs within the inlet region, being quite negligible outside that region.

Most experimental studies were performed to evaluate the stored water temperature profile and thermocline thickness development during the charging cycle in storage tanks [7–9]. Analytical and numerical models have been carried out to investigate the cited mechanisms over thermocline stability and tank loss of capacity [10–14].

Waluyo and Majid [15] developed an experimental parametric study to determine the "S-curve" and thermocline thickness during the charging regime for a chilled water storage tank. No hydrodynamic parameter was considered to obtain the temperature distribution profile.

The same mechanism can be verified inside solar plant thermal storage tanks. Altuntop et al. [16] verified numerically thermocline instability due to convective flow and experimentally the effect of internal obstacles on the thermocline instability during hot water charging and discharging regimes.

Based on the work presented by previous authors [10–16], it is clear that the incoming flow regime generated by diffusers is a key parameter that affects the tank loss of capacity, giving rise to the thermocline instability phenomenon.

However, there is an additional tank loss of capacity which has been previously overlooked in the open literature to the authors' knowledge, which cannot be neglected at all when sizing a vertical tank: the loss caused by the mixing of water masses due to the viscous flow along the tank height. Typically, it is implicitly assumed that the downward flow is inviscid, a hypothesis that cannot be held in practical applications. For the study, the effects of this viscous flow can be noticed only out of the region influenced by the inlet diffuser, as the fluid velocity becomes essentially axial and the hydrodynamic boundary layer has started to develop.

This work establishes a method of estimating this new loss of capacity and provides working examples in which the consideration of the loss of capacity due to inlet diffuser only can lead to lower tank sizing.

2 Aspects for sizing a thermal storage vertical tank

For a particular tank, water and tank thermal capacity calculations along with an estimation of heat losses through tank wall and connections must be considered for sizing and a proper operation. The usual technique consists in determining the overall chilled water volume to be stored, along with tank geometrical aspects (height and diameter), to supply the total amount of chilled water for the air-conditioning system during the operation period.

2.1 Chilled water useful volume capacity

The useful tank storing volume capacity is determined from the total amount of internal energy that will be stored up by the water mass that fills up the tank. The total internal energy depends on the load demand profile of the air-conditioning system. In an ideal situation, in which there is not any heat loss, chilled water leaves the tank at temperature T_c and, after receiving the thermal load from the air-conditioning system, it returns back to the tank top at temperature T_h. Therefore, it is straightforward to show that the necessary useful tank volume V_u for supplying chilled water daily demand is given by Eq. (1):

$$V_u = \sum E_i / \rho\, c\, (T_h - T_c), \tag{1}$$

where E_i is the internal energy due to the difference between the thermal load and chiller capacity at a given time interval t_i of the thermal load profile; ρ and c are the density and the specific heat of the chilled water, respectively. Adopting a value for the tank diameter, it is simple to obtain the tank height, H_u. As an example, Fig. 1 illustrates an ideal the discharge history of a vertical tank for an installation of thermal storage for a 3 h period assuming no tank heat losses. If no mixing or viscous effects occur, then an ideal contact surface will separate the chilled water mass from the warm one, as indicated in that figure. As chilled water at the bottom is drawn out, the whole mass of water flows down uniformly within the tank as the warm water makes up at the top. Therefore, the contact surface moves downwards flat keeping the separation between the two water portions. The ideal contact surface will be used as a reference for accounting for other effects further on in this work.

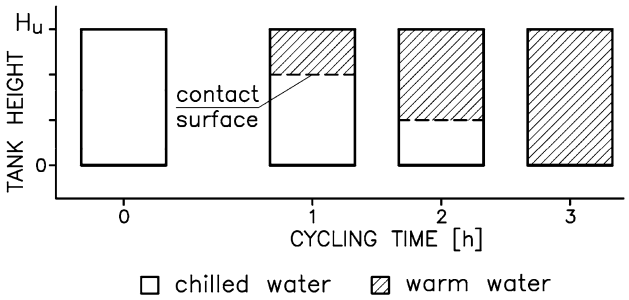

Fig. 1 Ideal discharge cycle of a thermal storage vertical tank with no viscous effects

2.2 Loss of storing capacity

Tank storing loss of capacity can be classified according to external and internal losses. External losses are those that cause undesirable increase of the air-conditioning system thermal load and they occur mainly due to heat infiltration from the surroundings into the stored chilled water. Heat infiltration can be minimized using good thermal insulation practices. On the other hand, internal losses are those that decrease the tank overall capacity and their main sources are: (1) warm and chilled water mixing, (2) heat conduction between the warm and chilled water through the tank wall ("thermal bridge"), (3) heat conduction between the chilled and warm water portions.

2.2.1 Loss of capacity due to chilled and warm water mixing

Among the several losses, the major loss is the one due to water mixing as illustrated in Fig. 2, whose resulting phenomenon is the thermocline undesireble problem, as previously mentioned in ASHRAE [3, 4]. In that figure, the thermocline zone represents the volume of water in which the temperature gradient occurs between the warm and the chilled water temperature. The dashed line within the thermocline zone represents the position of an ideal contact

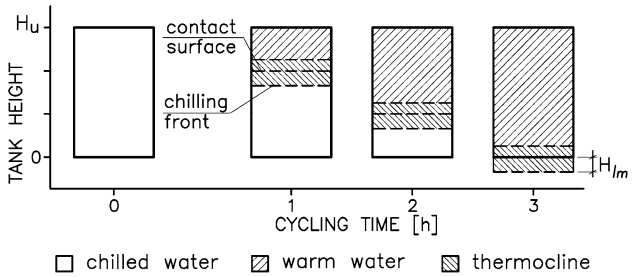

Fig. 2 Thermocline development in a vertical tank during the discharge cycle

surface that would be formed if there were no water mixing at the end of a working cycle. An amount of water in the thermocline zone with an H_{lm} height was used by the air-conditioning system, having a higher temperature than that of T_c. From the installation point of view, the air-conditioning performance will be degraded.

The term H_{lm} is defined as an equivalent height loss and it is of great concern to keep it as minimum as possible by designing diffusers to minimize water mixing and stirring at the tank inlet. H_{lm} must be added to the useful height H_u, which represents the tank height and the amount of chilled water, so that one can guarantee the supply of chilled water at the proper temperature.

Bahnfleth and Musser [7] present a set of working equations to estimate the loss of capacity in tanks that use the radial diffuser technology. Bahnfleth et al. [8, 9] present working equations to estimate the loss of capacity for octagonal diffuser; it is worth remarking that, by applying the Eqs. (4–14) proposed in [9] to a 0.0375 $m^3\ h^{-1}$ tank discharge flow, with a supply (T_c) and return (T_h) temperatures of 277.15 and 288.15 K, respectively, one obtains practically the same value for the loss of capacity for tanks whose diameters are in the range between 6 and 12.7 m, i.e., it was possible to combine the mentioned equation in dimensionless parameters to make the loss of capacity practically independent on the tank diameter [17]. A puzzling question arises from that fact: for storing the same water volume, a 6 m diameter tank would have a useful height about 4.5 times greater than that of a 12.7-m diameter tank. At the same time, for the smaller tank diameter, the Reynolds number based on the tank diameter, $Re_{Ø}$, would practically be twice the Reynolds number of the larger tank, for the same mass flow rate. Hence, the following question can be raised: has the water flow no influence at all over the tank performance and capacity? That point is addressed in next subsection.

2.2.2 *Loss of capacity due to water flow*

Figure 2 shows the ideal and the chilled front contact surfaces of the gradient temperature zone moving downwards at a constant velocity. However, in an actual situation, wall friction due to water viscosity will create a hydrodynamic boundary layer giving rise to a cross-sectional velocity dependency on the radial position. Therefore, the fluid portion closer to the central region (core) will be accelerated, while the fluid layer right in contact with the tank wall will be at rest as it is well known from the classical boundary layer analysis for internal flows. To illustrate further the problem, suppose an initial flat contact surface between the warm and the chilled water; next, the fluid starts moving downwards as depicted in Fig. 3. Assuming that there is no water mixing, the preceding flat contact surface will distort itself, as liquid in the core region is accelerated while the fluid portion next to the wall slows down due to viscous action.

At the end of a discharge cycle, some of the warm water will eventually flow out of the tank, whose volume is proportional to the height H_{lb}. Such an undesired effect is, therefore, somewhat similar to the mixing due to the diffuser discussed previously. To take that into account, let one define height H_{lb} as being an additional loss of capacity.

In an experimental work, Al-Marafie [18] verified the influence of hydrodynamic effects on thermocline. A tank having 3.2 m height and 1.7 m diameter was tested for determination of extraction efficiency (η_d) defined as the percentage ratio of the non-disturbed volume (undisturbed volumes above and under the established thermocline region) to the total tank volume for both the charging and the discharging processes. Results showed that the extraction efficiency for both the charging and the discharging process was in the range 86–91 %. Those figures indicate that stratified tanks can be effectively used for load management application in air-conditioning applications; the flow rate deviation from the design conditions (0.49, 0.74 and 1.06 l $kg\ s^{-1}$) caused a significant change in the disturbed zone thickness; and the inlet temperature to the tank for the charging or the discharging has little effect on the disturbed zone thickness.

In other experimental work, Nelson et al. [19] tested a 1,890 mm height by 540 mm internal diameter tank, in which the effects of mixing at the inlet, leading to the

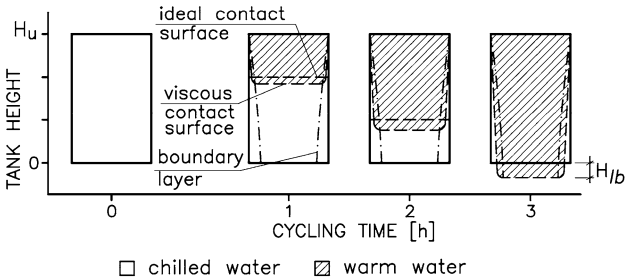

Fig. 3 Vertical tank loss of capacity during the discharge cycle due to boundary layer development

definition of the mixing coefficient were evaluated by a parametric analysis varying the aspect ratio (2–3.5), flow rates, initial temperature difference (10–15 K), and thickness of insulation (0.1 and 0.2 m) during charging and discharging cycles. They sought to obtain a mixing coefficient expressed as a function of Re and Ri to eliminate the usage of adjustable empirical parameters for predicting the temperature profiles. Regarding performance improvement with height to diameter ratio parameter, those authors concluded that it is not significant beyond height to diameter ratio of about 3. Concerning thermal stratification, it does not improve much for length-to-wall thickness ratios >200 for any tank. Another important conclusion was that the percentage of chilled water recoverable in a discharge cycle increased with increasing the initial temperature difference, aspect ratio, and flow rate. The charge and discharge efficiencies increased with increasing flow rate and initial temperature difference.

2.2.3 Overall tank height

Once a given tank diameter is chosen, after project design and site availability considerations, the overall tank height is promptly obtained by the useful volume added to the volume corresponding to the losses of capacity described in Subsect. 2.2.1 and 2.2.2. Therefore, by adding up the combined extra height (notice, however, that H_{lm} and H_{lb} cannot be independently added) to trade off for the thermocline zone and water boundary layer extension, the chilled water always has to be delivered at T_c. Section 3 addresses the subject on how to evaluate the later loss of capacity, i.e., due to the viscous effect associated with water flow inside the tank.

3 Hydrodynamic boundary layer effect over the tank performance

As seen in previous section, tank losses of capacity are usually assumed to originate from the diffuser alone. However, the present analysis shows that the boundary layer growth can actually be the dominant effect on degrading the tank performance and this subject will be approached next.

3.1 Methodology of this work

Figure 3 depicts the problem of the contact surface distortion and the source of the additional loss of capacity due to the hydrodynamic boundary layer growth for both a laminar and a turbulent flow. The proposal is to account for the boundary layer effect; H_{lb} should be represented by the difference between the ideal and the viscous contact surface tip positions at the axial line. Once those surface velocities are known, their instantaneous position can be determined and, consequently, the equivalent height loss due to such an undesirable phenomenon.

In "Appendix A", the analytical modeling of the boundary layer development used throughout this work is presented. As seen in Fig. 4, the laminar and turbulent flow regimes are analyzed. The distance from the tube entrance to the point boundary layer tip, called hydrodynamic entry length, was first made dimensionless in that figure, for comparing the boundary layer development.

To analyze the problem properly, the analysis is divided into two different cases: in the first one, the water flow regime is assumed to be laminar, and on the other, the flow regime is assumed to be turbulent. The laminar or turbulent boundary layer development will depend on the Reynolds number, as usual for internal flows.

3.2 Definitions

To carry out the study, let a dimensionless position f account for any fluid position computed from the boundary layer starting point, to be defined as:

$$f = x/x_{el} \tag{2}$$

In Fig. 5 it is possible to identify the main variables of the problem, namely: r_0: cylindrical tank internal radius; x: contact surface distance from the boundary layer beginning; δ: boundary layer thickness at distance x; x_{el}: hydrodynamic entry length.

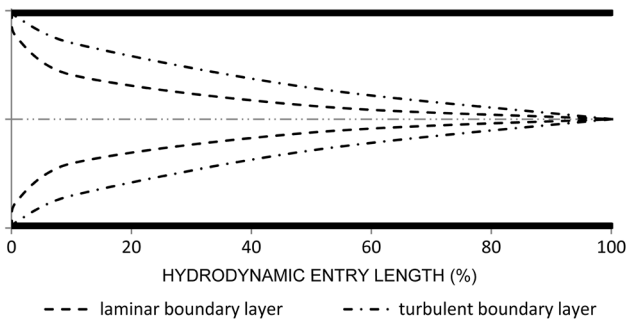

Fig. 4 Laminar and turbulent boundary layer development for internal flow in tubes

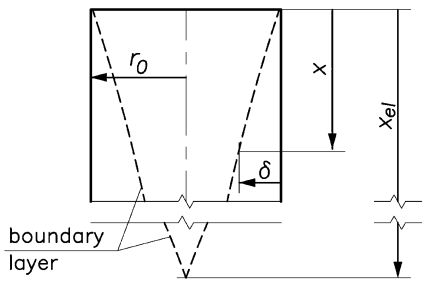

Fig. 5 Boundary layer relevant variables identification

Let also the ideal contact surface be the one that does not undergo any distortion as the water flows downward as already defined, i.e., there are no viscous effects. Such an ideal surface would move downwards at a velocity proportional to the instantaneous mass flow rate as if it were a rigid piston moving downwards the tank. On the other hand, viscous effects will distort that contact surface changing it into a viscous contact surface, due to the hydrodynamic boundary layer development, as already discussed.

3.3 Laminar flow analysis

Laminar flow inside tubes is defined for a Reynolds number, $\mathrm{Re}_{\emptyset}$, based on the tube diameter, ϕ, <2,300 [20, 21]. For the boundary layer analysis, let one consider the following assumptions: (1) steady-state situation, (2) there is no water mixing due to the diffuser, i.e., a (viscous) contact surface will form between the warm water introduced into the tank and the stored chilled one, (3) the flow is uniform and the boundary layer starts to develop at the tank top edge, (4) heat conduction transfer is neglected, (5) gravitational effects are also neglected, except for temperature stratification.

With respect to Fig. 6, axial velocity U at the center line is given by:

$$U = \frac{\mathrm{d}x_{\mathrm{l}}}{\mathrm{dt}} \tag{3}$$

Differentiating Eq. (2) (with constant discharge flow), substituting the result into Eq. (3) and carrying out some manipulations, one obtains:

$$\frac{\mathrm{d}t}{x_{\mathrm{ell}}} = \frac{\mathrm{d}f}{U} \tag{4}$$

where index "l" has been added to the length x and x_{el} to identify entrance length as a laminar flow.

The entrance length x_{ell} can be calculated by the Langhaar equation in Kays and Crawford [21]:

$$x_{\mathrm{ell}} = 0.05\phi\mathrm{Re}_{\phi} \tag{5}$$

Warm water on the top of chilled water the tank both flow downwards during the discharge process. Because $\mathrm{Re}_{\emptyset}$ is temperature dependent, then two different values of $\mathrm{Re}_{\emptyset}$ are obtained. Equation (5) requires a value for $\mathrm{Re}_{\emptyset}$ to calculate the hydrodynamic entry length. The chilled water, owning a lower $\mathrm{Re}_{\emptyset}$, has a shorter entry length, due to the faster radial velocity profile development. However, at the contact surface, it cannot have two different radial velocity distributions, because it would result in two values for the water flow in the same area. Therefore, the hydrodynamic entry length for chilled water must prevail and, then, the $\mathrm{Re}_{\emptyset}$ calculated using the transport properties of chilled water will be used in Eq. (5).

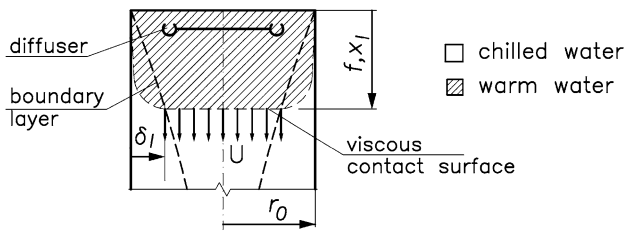

Fig. 6 Laminar boundary layer relevant variables identification

In laminar flow, U can be related to f by means of the following equation (as shown in "Appendix A"):

$$U/U_0 = (373f + 1)^{0.1} \tag{25}$$

being U_0 the mean velocity. Equation (A.2) is valid for $f < 0.1$ and $400 < \mathrm{Re}_{\emptyset} \leq 2{,}300$. Therefore, (4) becomes:

$$\frac{U_0}{x_{\mathrm{ell}}}\mathrm{d}t = \frac{\mathrm{d}f}{(373f + 1)^{0.1}} \tag{6}$$

In Eq. (6), the analytical solution is valid for the case in which U_0 and x_{ell} are held constant at each time step. That is possible, once the thermal load (and consequently the discharge flow) is usually considered to be constant at each 1 h interval, which is a typical interval in any thermal load profile. Therefore, by assuming a discharge flow as being constant within two instants t_1 and t_2, the analytical solution of Eq. (6) is given by Eq. (7):

$$\frac{U_0(t_2 - t_1)}{x_{\mathrm{ell}}} = \left[\frac{(373f + 1)^{0.9}}{335.7}\right]_{f_1}^{f_2} \tag{7}$$

By applying Eq. (7) at each time interval i, in which the discharge flow is constant, one obtains:

$$\frac{U_{0,i}\left(t_{2,i} - t_{1,i}\right)}{x_{\mathrm{ell},i}} = \left[\frac{(373f + 1)^{0.9}}{335.7}\right]_{f_{1,i}}^{f_{2,i}} \tag{8}$$

In Eq. (8), $f_{1,i}$ and $f_{2,i}$ are the initial and final position of the viscous contact surface tip at the center line during the time step considered. The numerator on the left-hand side can be interpreted as the displacement of a fluid particle for the ideal case of a flat contact surface. Therefore, at each time interval, the displacement of the ideal contact surface is given by:

$$\Delta x_{0,i} = U_{0,i}\left(t_{2,i} - t_{1,i}\right) \tag{9}$$

The overall ideal contact surface displacement, $x_{0\mathrm{l}}$, after n time intervals, results from the overall sum of each individual displacement, i.e.,:

$$x_{0\mathrm{l}} = \sum_{i=1}^{n} \Delta x_{0,i} \tag{10}$$

The displacement of the viscous contact surface tip, $\Delta x_{\mathrm{l},i}$, at each time interval i is:

$$\Delta x_{l,i} = \left(f_{2,i} - f_{1.i}\right) x_{\mathrm{ell},i} \tag{11}$$

The overall displacement, x_{lo}, of the viscous contact surface tip will be:

$$x_{\mathrm{lo}} = x_{l,n} = f_{2,n}\, x_{\mathrm{ell},n} \tag{12}$$

As the hydrodynamic entry length in laminar flow is very large, the viscous boundary layer is considered to starts developing at the tank top; $x_{0\mathrm{l}}$ and x_{lo} are, respectively, the overall ideal and actual tank height, given by the ideal and viscous surfaces. The loss of capacity due to hydrodynamic boundary layer effects can be defined as the difference between the viscous contact surface displacement and the ideal contact surface one. Let H_{lbl} be defined as that difference:

$$H_{\mathrm{lbl}} = x_{\mathrm{lo}} - x_{0\mathrm{l}} \tag{13}$$

3.4 Turbulent flow analysis without initial loss of capacity

The procedure for analyzing the boundary layer effects in turbulent flow is analogous to the one for laminar flows. The simplifications listed in Sect. 3.2 are also valid, except the assumption (3). The equation that correlates axial velocity U to dimensionless length f, considering that the boundary layer starts as a turbulent one, is given by (Eq. 14):

$$U/U_0 = (17.8f + 1)^{0.08} \tag{14}$$

This equation is valid for $f < 0.9$ and $\mathrm{Re}_{\varnothing} \geq 4{,}000$. Differentiating Eq. (2) (with constant discharge flow), substituting the result into Eq. (3), and carrying out a few manipulations, one obtains:

$$\frac{\mathrm{d}t}{x_{\mathrm{elt}}} = \frac{\mathrm{d}f}{U} \tag{15}$$

where index "t" has been added to the entry length x and x_{el} to identify it as a turbulent flow.

From Eqs. (15) and (14), one obtains:

$$\frac{U_0}{x_{\mathrm{elt}}}\mathrm{d}t = \frac{\mathrm{d}f}{(17.8f + 1)^{0.08}} \tag{16}$$

The hydrodynamic turbulent entry length x_{elt}, considering that the boundary layer starts as turbulent from the top, can be calculated using Latzko's equation [21]:

$$x_{\mathrm{elt}} = 0.623\phi \mathrm{Re}_{\phi}^{1/4} \tag{17}$$

Equation (16) can only be integrated within each time interval where U_0 and x_{elt} are constants, i.e., where the discharge flow is constant. Therefore, by considering the discharge flow as being constant within two instants t_1 and t_2, the solution of Eq. (16) becomes:

$$\frac{U_{0,i}\left(t_{2,i} - t_{1,i}\right)}{x_{\mathrm{elt},i}} = \left[\frac{(17.8f + 1)^{0.92}}{16.376}\right]_{f_{1,i}}^{f_{2,i}} \tag{18}$$

For the ideal displacement, Eq. (9) is still valid. The hydrodynamic contact surface displacement $\Delta x_{t,i}$, at each time interval i is:

$$\Delta x_{t,i} = \left(f_{2,i} - f_{1.i}\right) x_{\mathrm{elt},i} \tag{19}$$

The viscous contact surface displacement, from the beginning of the boundary layer, is:

$$x_{t0} = x_{t,n} = f_{2,t}\,.\,x_{\mathrm{elt},n} \tag{20}$$

In turbulent flows, water is not introduced with a uniform velocity over the cross sectional area at the tank top; thus, the boundary layer does not start to developing right at the beginning. Once the hydrodynamic entry length is now substantially shorter than that of laminar flows, the hypothesis that boundary layer starts at the tank top edge becomes inappropriated. Based on the fact previously mentioned that the entry diffuser influence is negligible after three meters from the tank top [3], so that the flow will be considered to become uniform after that length (let us call it L), where the turbulent boundary layer starts developing as illustrated in Fig. 7.

The overall ideal contact surface displacement is the sum of each n individual plus the distance from the tank top to the boundary layer beginning (length L), i.e.,:

$$x_{0t} = \sum_{i=1}^{n} \Delta x_{0,i} + L \tag{21}$$

The equivalent height loss due to boundary layer is:

$$H_{\mathrm{lbt}} = x_{t0} + L - x_{0\mathrm{l}} \tag{22}$$

Working example 1: for a thermal storage system, with 0.0375 m^3/s discharge constant flow having a 3 h cycling time, a 6 m tank diameter and $\mathrm{Re}_{\varnothing}$ equal to 5,068, the loss equivalent height due to water flow is 1.32 m. To calculate that loss, notice that the viscous contact surface moves downwards at the mean velocity flow for the first three meters from the tank top, lasting 2,262 s to cover such distance, before reaching the velocity field given by Eq. (14). Only after that, Eq. (18) can be used to determine the remaining displacement. Figure 8 shows the results of a

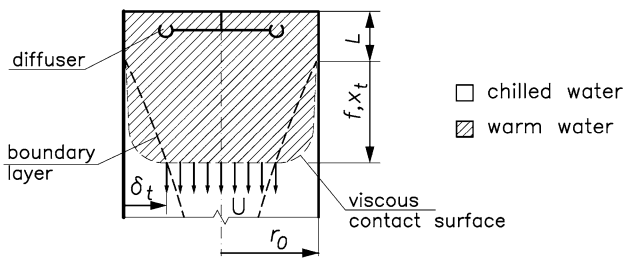

Fig. 7 Turbulent boundary layer relevant variables identification without any initial loss of capacity

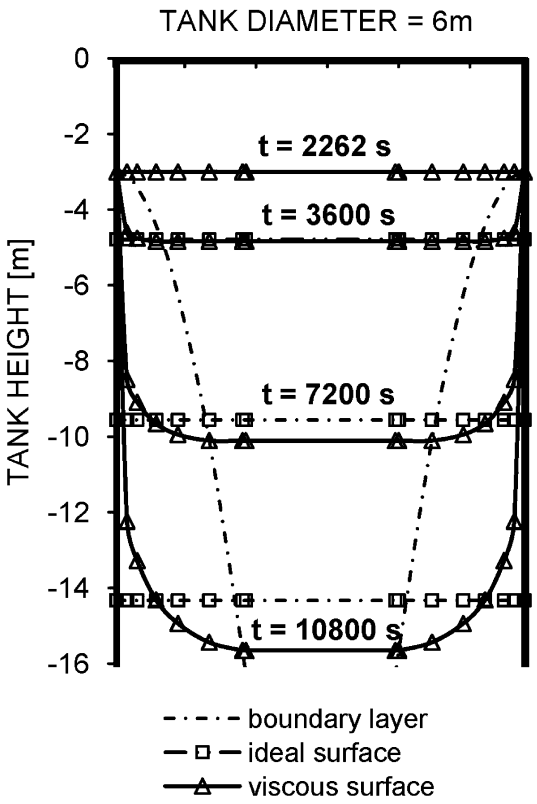

Fig. 8 Displacement of the ideal and viscous contact surface for a 3-h cycling time at constant flow ($Re_{\varnothing} = 5068$)

calculation for the ideal and viscous surface displacements down the tank height, for the given example.

3.5 Full thermal storage: turbulent flow with initial loss of capacity

As already mentioned, when warm water is introduced into the tank, it causes a partial water masses mixing. The equivalent height loss due to that mixing, H_{lm} (see Fig. 2), therefore, should be considered in the tank performance analysis.

Figure 9 illustrates the proposed situation. In the case of no mixing, the useful chilled water would be immediately below the viscous contact surface, as depicted in Fig. 7. Once the mixture occurs, let us consider that an ideal contact surface will also occur, which in this situation is represented by the dashed line. The useful non-disturbed water right below the surface has been identified as (thermocline) chilling front. The distance between the chilling front and the ideal contact surface, being H_{lm} at the beginning, will always be the total equivalent height loss.

Working example 2: let one consider the same situation of working example 1, except by the initial height loss due to the inlet diffuser (H_{lm}) set now at 1.0 m. From previous example, the height loss due to water flow ($H_{lb(t)}$) was

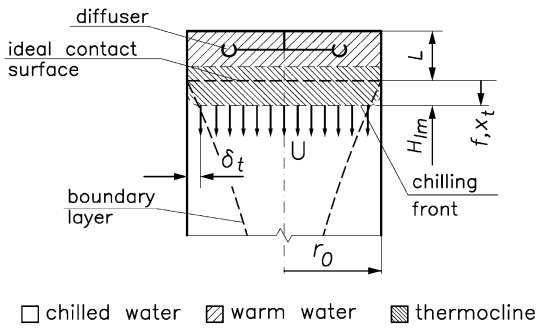

Fig. 9 Turbulent boundary layer relevant variables identification with initial mixing of water masses

1.32 m; the added two height loss is 2.32 m. Now, however, one has to consider the temperature chilling front in place of the viscous contact surface. Once the chilling front has advanced 1 m from the viscous surface, it has a higher initial velocity and it is displaced by a 1.48 m in length. The combined height loss will be 2.48 m, while the sum of the effects would be 2.32 m. It shows H_{lm} and H_{lb} are not additive, i.e., they cannot be merely added to one another.

4 Discussion

4.1 Flow characteristics

For water downward flows in the tank, a simplified model was adopted, in which no water mass mixing was considered and the effect of density difference was neglected, except for the formation of a temperature stratification zone. Figure 8 illustrates the result for that model. Notice that inside the hydrodynamic boundary layer chilled water column is established, keeping the warm water out by means of a contact surface.

However, that viscous effect is observed to make the chilled water inside boundary layer move across the boundary layer (and thus through the contact surface) into the core at the tank center line, causing mixing of chilled and warm waters. The viscous effects, therefore, cause the mixing of water masses all along the discharge cycle period. The mixing effect occurs above the viscous contact surface (or the thermocline chilling front, depending on the case considered). In addition, gravitational effects due to difference of water density act in the same direction as the viscous effect.

4.2 The turbulent hydrodynamic entry length

This work used the turbulent hydrodynamic entry length, calculated from Eq. (17), suggested by Latzko [21], which considers the turbulent boundary layer development starting at the beginning of fluid inlet in pipes. As a simple rule

of thumb, a considerable part of the specialized literature adopts the turbulent hydrodynamic entry length to be ten times the tube diameter. According to Eq. 17, such result will only reach that rule for $Re_{Ø} > 66{,}000$, which exceeds typical values of a thermal storage tank. Shah and Sekulic [22] suggest the following equation, for $Re_{Ø}$ starting from 10,000:

$$x_{elt} = 1.359\phi Re_{\phi}^{1/4} \quad (23)$$

However, for reaching that length, the flow starts as a laminar boundary layer, progressively going through the transition regime and, finally, reaching the turbulent regime. It requires a smooth tube entrance, with a quite uniform velocity flow over the cross-sectional area and without any other turbulence or tube flow disturbance. Such conditions are not characteristic of the flow in thermal storage tanks. Also, the gravity effect has not been taken into account as it is not considered by the entry length equations given by the aforementioned authors.

5 Conclusions

(a) Viscous effects cause the viscous contact surface to forerun the ideal contact surface at the tank center line and to slow the fluid down at regions near the tank wall. That phenomenon causes a loss of storing capacity and should be considered by sizing the overall tank height, so that warm water does not reach the outlet diffuser until the discharge cycle ends. The Reynolds number based on tank diameter $Re_{Ø}$, and parameter f, defined in Eq. (2), which relates the viscous contact surface of the water masses (simplified model) or the temperature chilling front (actual case) with the hydrodynamic entry length have been the fundamental parameters for the realistic study of the loss of capacity.

(b) The idea that "a tall tank is desirable for stratification […]" as suggested in reference [3] should be carefully reconsidered. Based on such assertive, one may be misled to adopt a smaller tank diameter if the situation requires less installation space in the plant. Depending on the case, the decision for a taller tank can lead to an equivalent height loss many times higher than the estimated one, based only on losses due to the diffuser alone [23]. Viscous boundary layer development in flows inside vertical thermal storage tanks can be extremely harmful to the efficiency of the system. Even in laminar flows, whose hydrodynamic entry length is generally very high, the boundary layer influence can be substantial.

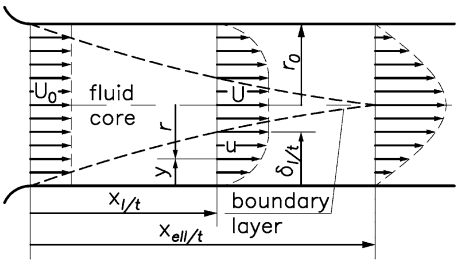

Fig. 10 Velocity profile along the hydrodynamic entry length

Table 1 Axial velocity at fluid core and boundary layer thickness along the hydrodynamic entry length—laminar flow inside tubes

$(x_l/Ø)/Re_{Ø}$	f	δ/r_0	U/U_0^b	U/U_0 Eq. (25)	Deviation (%)
0	0	0	1	1	0
0.0005	0.01	0.254	1.1503	1.168	+1.54
0.005	0.1	0.592	1.4332	1.440	+0.47
0.0225	0.45	0.877	1.8240	1.670	−8,44
0.05[a]	1	1	2	1.809	−9.6

[a] Value obtained from the Langhaar equation [21]

[b] Value obtained from the Hornberk's studies [24]

Appendix A: Correlations for axial velocity along with the hydrodynamic entry length flow inside tubes and flat plates

As a liquid flows inside a cylindrical thermal storage tank, a hydrodynamic boundary layer is formed next to the wall due to viscous effects, giving rise to velocity gradients across the tank section, as depicted in Fig. 10. Outside that boundary layer (fluid core), viscous effects are negligible and the fluid flows with uniform velocity, which increases as the boundary layer grows thicker, due to the mass conservation law. As well known, two flow regimes can be formed and they are reviewed next in the context of the present work.

Laminar flow

Laminar flow inside tubes occurs for a Reynolds number based on tube diameter, $Re_{Ø}$, less or equal to 2,300, as well established in Fox et al. [20] and Kays and Crawford [21]. Table 1 shows the values for axial velocity at the fluid core along with the boundary layer thickness given as a function of the distance x_l from the beginning of the boundary layer formation. The data have been extracted from the studies of Hornbeck [24], being valid for $Re_{Ø}$ higher than 400.

Hornbeck's solution [24] requires $(x_l/Ø)/Re_{Ø}$ going to infinity for reaching the fully developed flow condition. However, according to Langhaar [21], hydrodynamic entry length x_{ell} can be determined by Eq. (24):

$$\frac{x_{ell}/\phi}{Re_{\phi}} = 0.05, \quad Re_{\phi} \leq 2,300 \tag{24}$$

Hence, in the first column in Table 1 the value of Eq. (24) was used for $(x_l/Ø)/Re_Ø$. In the second column, f represents the dimensionless boundary layer distance considered from the beginning of the boundary layer formation, as defined in Eq. (2).

Usually, the hydrodynamic entry length is greater than the usual thermal storage tank height and, therefore, the inside flow never reaches the fully developed flow regime. Using Eq. (24) for $Re_Ø$ equals to 2,300, for example, one has x_{ell} equal to 115 Ø. If one considers a particular tank with 15 m diameter and 20 m high, the dimensionless length for the height will be equal to 0.01. Therefore, a correlation which represents the values of the axial velocity from the studies by Hornbeck [24] for a f range between 0 and 0.1 as well as possible should be sought. A correlation that meets such conditions is given below:

$$U/U_0 = (373f + 1)^{0.1} \tag{25}$$

The last two columns in Table 1 show the axial velocity calculated from Eq. (25) and the relative deviation, when compared to the values from the studies by Hornbeck [24]. As observed, the values obtained are very reasonable for the considered f range.

Turbulent flow

The turbulent flow inside tubes is well defined for the Reynolds number based on tube diameter, $Re_Ø$, equal or higher than 4,000 [19, 20]. For the flow within the hydrodynamic entry length, the equation relating a given length x_t with the axial velocity at the fluid core will be obtained from some analogies with the flow over a flat plate. For the velocity in the fully developed flow, the power law profile was used, with the exponent equal to 1/6, which represents the velocity radial distribution in turbulent flow for $Re_Ø$ equals to 4,000. The other acceptable exponent value is 1/7 that is valid for $Re_Ø$ equals to 110,000 [6], which greatly exceeds the typical Reynolds number values of the thermal storage tank. For flow over a flat plate, the power law profile with the exponent 1/6 was also used. Table 2 shows a summary of relevant Eq. (27) through (30) for flow over flat plates and inside tubes, set side by side, needed for Milaré's study of analogies [17]. The relative nondimensional thickness δ^* can be defined as the ratio between the boundary layer thickness (within the reference length) and the reference thickness, as it can be seen in Eq. (26):

$$\left(\frac{\delta^*_t}{\delta^*_l}\right)_{\text{flat plate}} = f^{0.3} \tag{26}$$

where indexes "l" and "t" have been added to δ^* to identify laminar and turbulent flow.

Analogies between flow over a flat plate and inside tube

Equations for flows over a flat plate and inside a tube are similar and two possible analogies are usually used for describing them, as discussed next.

First analogy

For the laminar regime, let one adopt the velocity profile of the flat plate to represent the velocity radial distribution inside the boundary layer, along with the hydrodynamic entry length inside tubes. It is first necessary to verify if the velocity profile of the fully developed flow is met. Making δ in Eq. (28) equal to r_0 (when the flow becomes fully developed, the boundary layer thickness grows to the tube ratio) and y equal to $(r_0 - r)$, one obtains Eq. (32). The second step is to verify if applying Eq. (28) inside the boundary layer, at a given cross section within the entry length, along with the equation of continuity, one obtains the axial core velocity value equal to the values obtained from the studies by Hornbeck [24]. In fact, the values obtained for axial velocities are quite close to the ones obtained from Hornbeck' studies as shown in the last column in Table 1 (less than 3 % deviation for the range of interest and less than 6 % for the entire range). Therefore, for laminar flow inside tubes and within the hydrodynamic entry length, Eq. (28) can represent the velocity inside the laminar boundary layer.

Table 2 Equations for flows over flat plate and inside tubes

Regime	Subject	Flat plate	Tube
Laminar	Entry length[a]	$x_{el} = 0.04\ \frac{U_0\delta_{el}^2}{\nu}$ (27)	$x_{ell} = 0.05\ \frac{U_0\phi^2}{\nu}$ (31)
	Velocity profile[b]	$\frac{U}{U_0} = 2\frac{y}{\delta_l} - \left(\frac{y}{\delta_l}\right)^2$ (28)	$\frac{U}{U} = 1 - \left(\frac{r}{r_0}\right)^2$ (32)
Turbulent	Entry length[a]	$x_{et} = 5,186\left(\frac{U_0\delta_{et}}{\nu}\right)^{1/4}\delta_{et}$ (29)	$x_{elt} = 0.623\left(\frac{U_0\phi}{\nu}\right)^{1/4}\phi$ (33)
	Velocity profile[b]	$\frac{U}{U_0} = \left(\frac{y}{\delta_t}\right)^{1/6}$ (30)	$\frac{U}{U} = \left(1 - \frac{r}{r_0}\right)^{1/6}$ (34)

[a] For flow over flat plate, it refers to the reference length

[b] For flow inside tubes, it refers to full developed flow

Table 3 Axial velocity at fluid core and boundary layer thickness along the hydrodynamic entry length—turbulent flow inside tubes

f	δ/r_0	U/U_0 (analogies)	U/U_0 Eq. (36)	Deviation (%)
0	0	1	1	0
0.01	0.062	1.018	1.013	−0.5
0.1	0.297	1.085	1.085	0
0.45	0.712	1.197	1.192	−0.42
1	1	1.264	1.264	0

By comparing equations for turbulent flow over a flat plate and inside a tube, one can notice that they are very similar to each other in a similar fashion to the ones for the laminar flow case. Also, if one assumes in Eq. (30) the same simplifications assumed in Eq. (28) for the laminar case, one obtains Eq. (34). Therefore, as the first analogy, Eq. (30) will be assumed to represent the velocity radial distribution inside the boundary layer for the hydrodynamic entry length for turbulent flow inside tubes.

Second analogy

Analyzing Table 2, the particularity between Eqs. (27) and (29) (flow over a flat plate) is verified to be very similar to the particularity between Eqs. (31) and (33) (flow inside tubes). And so is the relationship between Eqs. (28) and (30) to the particularity between Eqs. (32) and (34). From these comparisons, as the second analogy, the relation between the relative thickness and the dimensionless length for flows over flat plate, Eq. (26), will be assumed to be also valid for flows inside tubes. Therefore:

$$\left(\frac{\delta^*_t}{\delta^*_l}\right)_{\text{inside tubes}} = f^{0.3} \tag{35}$$

Correlations for axial velocity at fluid core inside the tube

From the above analogies and the values from Table 3, one can obtain, along with the equation of continuity, the values for axial velocity and relative thickness, as a function of the dimensionless position f from the beginning of the boundary layers, for turbulent flow.

The hydrodynamic entry length in turbulent flow is far smaller than that of the laminar one. Using Eq. (16) $\text{Re}_{\text{Ø}}$ equal to 5,000, for example, one has x_{elt} equal to 5.23 Ø. If one considers the same tank from the laminar example, the dimensionless length for the height will be equal to 0.255. However, larger values of f are possible.

Therefore, a correlation that represents the values of the axial velocity for a largest f range as well as possible should be sought. A correlation that meets such a condition is given below:

$$U/U_0 = (17.8f + 1)^{0.08} \tag{36}$$

The last two columns in Table 3 show the axial velocity calculated from Eq. (36) and the relative deviation, when comparing those results with the values from the analogies. As observed, the values obtained from that equation are very reasonable for the entire f range. However, Eq. (36) does not obey one boundary condition, that is: its derivative relative to f, for f equals 1, should be zero, but it does not vanish. Its application should thus be limited, say, for f in the range between 0 and 0.9.

References

1. Patin A, Defude J, Patry J (1985) Thermal conditioning through intermediary fluid and latent power storage. Int J Refrig 8:17–21
2. Saito A (2002) Recent advances in research on cold thermal energy storage. Int J Refrig 25:177–189
3. ASHRAE Handbook (2003) Heating, ventilating, and air-conditioning applications. Am. Soc. Heating, Refrig. Air-Conditioning. Engineers Inc., I-P Ed. 34
4. ASHRAE Handbook (2011) Heating, ventilating, and air-conditioning applications. Am. Soc. Heating, Refrig. Air-Conditioning. Engineers Inc., I-P Ed. 34
5. Li G, Hwang Y, Radermacher R (2012) Review of cold storage materials for air conditioning application. Int J Refrig 35:2053–2077
6. Wildin MW, Sohn CW (1993) Flow and temperature distribution in a naturally stratified thermal storage tank. USACERL technical report FE-94/01 37
7. Bahnfleth WP, Musser A (1998) Thermal performance of a full-scale stratified chilled-water thermal storage tank. ASHRAE Trans 104:12
8. Bahnfleth WP, Song J, Cimbala JM (2003) Measured and modeled charging of stratified chilled water thermal storage tank with slotted pipe diffuser. HVAC&R Res 9:467–492
9. Song J, Bahnfleth WP, Cimbala JM (2004) Parametric study of single-pipe diffusers in stratified chilled-water storage tanks (RP-1185). HVAC&R Res 10:345–365
10. Bahnfleth WP, Song J (2005) Constant flow rate charging characteristics of a full-scale stratified chilled water storage tank with double ring slotted pipe diffuser. Appl Ther Eng 25:3067–3082
11. Safi MJ (1994) Development of thermal stratification in a two-dimensional cavity: a numerical study. Int J Heat Mass Transf 37:2017–2024
12. Musser A, Bahnfleth WP (2001) Parametric study of charging inlet diffuser performance in stratified chilled water storage tanks with radial diffusers: part 1—model development and validation. HVAC&R Res 7:31–50
13. Musser A, Bahnfleth WP (2001) Parametric study of charging inlet diffuser performance in stratified chilled water storage tanks with radial diffusers: part 2—dimensional analysis, parametric simulations and simplified model development. HVAC&R Res 7:205–222
14. Chung JD, Shin Y (2011) Integral approximate solution for the charging process in stratified thermal storage tanks. Sol Energy 58:3010–3016
15. Waluyo J, Majid MA (2010) Temperature profile and thermocline thickness evaluation of stratified thermal energy storage tank. Int J Mech Mechatron Eng 10:7–12

16. Altuntop N, Arslan M, Ozceyhan V, Kanoglu M (2005) Effect of obstacles on thermal stratification in hot water storage tanks. Appl Ther Eng 25:2285–2298
17. Milaré MM (2009) Study of the influence of the hydrodynamic boundary layer over the chilled water thermal storage tank performance during the discharge cycle (in Portuguese). Dissertation, Universidade de São Paulo. http://www.teses.usp.br/teses/disponiveis/3/3150/tde-19052009-115422/
18. Al-Marafie AMR (1987) Stratification behaviour in a chilled water storage tank. Int J Refrig 10:364–366
19. Nelson JEB, Balakrishnan AR, Srinivasa Murthy S (1999) Experiments on stratified chilled-water tanks. Int J Refrig 22:216–234
20. Fox RW, McDonald AT, Pritchard PJ (2006) Introduction to fluid mechanics, 6th edn. Wiley, New York
21. Kays WM, Crawford ME (1993) Convective heat and mass transfer, 3rd edn. McGraw-Hill, New York
22. Shah RK, Sekulic DP (2003) Fundamentals of heat exchanger design. Wiley, New York
23. Wildin MW, Truman CR (1985) Evaluation of stratified chilled-water storage techniques. EPRI EM-4352 1–2:102
24. Hornbeck RW (1964) Laminar flow in the entrance region of a pipe. Appl Sci Res 13:224–232